Lattice Distortion Effects on the Magnetostructural Phase Transition of MnAs

F. Iikawa,[1,*] M. J. S. P. Brasil,[1] C. Adriano,[1] O. D. D. Couto,[1] C. Giles,[1,2] P. V. Santos,[3]
L. Däweritz,[3] I. Rungger,[4] and S. Sanvito[4]

[1]*Instituto de Física "Gleb Wataghin," UNICAMP, Campinas-SP, C.P. 6165, 13083-970, Brazil*
[2]*Laboratório Nacional de Luz Síncrotron, C.P. 6192, 13084-971 Campinas-SP, Brazil*
[3]*Paul-Drude-Institut für Festkörperelektronik, Hausvogteiplatz 5-7, 10117 Berlin, Germany*
[4]*Department of Physics, Trinity College, Dublin 2, Ireland*
(Received 22 March 2005; published 11 August 2005)

We present a systematic experimental and theoretical study of the first-order phase transition of epitaxially grown MnAs thin films under biaxial tensile stress. Our results give direct information on the dependence of the phase-transition temperature of MnAs films on the lattice parameters. We demonstrate that an increase of the lattice constant in the hexagonal plane raises the phase-transition temperature (T_p), while an increase of the perpendicular lattice constant lowers T_p. The results of calculations based on density functional theory are in good agreement with the experimental ones. Our findings open exciting prospects for magneto-mechanical devices, where the critical temperature for ferromagnetism can be engineered by external stress.

MnAs presents a first-order phase transition at $\sim 40\,°C$, changing from ferromagnetic/hexagonal (α-phase NiAs structure) to paramagnetic/orthorhombic (β-phase MnP structure) [1]. This magneto-structural phase transition has important implications for technological applications. The magneto-elastic effects are useful for transducers [2], while their magneto-caloric properties are interesting for developing refrigeration devices [3]. In recent years, the attention given to MnAs has been strongly amplified by the possibility of epitaxial growth on GaAs substrates [4]. The integration of ferromagnetic materials with semiconductors is a subject of great interest for spintronics, and MnAs grown on GaAs is a strong candidate for spin injection devices [5].

From the theoretical point of view, the treatment of the first-order phase transition of materials with magneto-elastic properties is a rather complex issue. Early simple phenomenological thermodynamic treatments based on the localized Heisenberg model [1] have been used to explain the properties of MnAs under an external hydrostatic pressure and magnetic field. Sophisticated band structure calculations are required for a precise quantitative analysis, although in this case it is difficult to introduce a statistical treatment to describe a first-order phase transition [6].

We present an experimental and theoretical investigation of the magneto-structural phase transition of MnAs films grown on GaAs. Those films present a nonabrupt phase transition with the coexistence [7] of the two phases in form of periodically alternating stripes [8,9] for a large temperature range ($\sim 20\,°C$) [7–10]. As a result of this phase coexistence a considerable fraction of the volume of the MnAs epitaxial films is usually in the paramagnetic phase at $\sim 30\,°C$, which is a strong limitation for room temperature spintronic devices. The growth of MnAs films on different crystal orientations has been suggested as an alternative that can provide higher phase-transition tem-

peratures [10]. The detailed mechanism that associates the crystal distortion (lattice parameter variation) with the phase-transition temperature is, however, still unclear, This issue was addressed in the early days by Menyuk *et al.* [11]. Recently, sophisticated *ab initio* methods pointed out the important role played by the p-d hybridization as the driving force of the MnAs first-order phase transition [12]. However, detailed calculations correlating the magneto-elastic first-order phase transition with the lattice parameter variation have not yet been reported.

In order to get more insight into the MnAs phase transition, we have designed an x-ray diffraction experiment and performed theoretical calculations to investigate in detail the dependence of the phase-transition temperature on crystal distortions. Experimental results show a clear variation of the phase-transition temperature of MnAs films due to the lattice distortions imposed by the substrate and by the application of an external biaxial stress. We observed that an increase of the unit cell volume does not necessarily result in an increase of the transition temperature, in contrast to the phenomenological model of Bean and Rodbell [1]. From accurate electronic structure calculations, we obtained a general and quantitative relationship between the exchange energy and the independent variation of each MnAs lattice parameter. We propose that the variation of the exchange energy can be associated with the MnAs phase-transition temperature. Based on this assumption, we were able to obtain a direct relationship between the phase-transition temperature and any MnAs lattice distortion, even though our calculations do not include a thermodynamic treatment of the phase transition. The validity of our approximation is corroborated by a good agreement between the experimental results and the theoretical predictions.

Our MnAs films are epitaxially grown on GaAs(001) by molecular beam epitaxy under growth conditions that yield
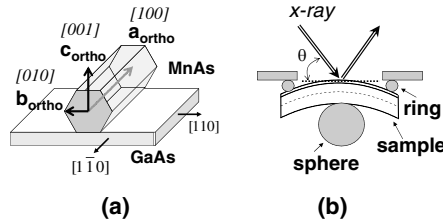
FIG. 1. (a) Schematic diagram of a unit cell of the
A-orientation MnAs/GaAs(001). The lattice parameters a_{ortho},
b_{ortho}, and c_{ortho} are defined in the orthorhombic structure nota-
tion. (b) Diagram of a biaxial stress ring cell. The x-ray beam
was focused at the center of the ring.

A-oriented films, [13] as shown in the Fig. 1(a). We use
here the orthorhombic notation [see Fig. 1(a)], which is
more appropriate for MnAs film on GaAs, since the films
are deformed by the substrate and lose the hexagonal
symmetry to an orthorhombic one even in the α phase.
The results presented here were obtained for a 130 nm
thick MnAs film. External biaxial strain was applied using
a stress ring cell [14] assembled in a temperature controlled
continuous N$_2$ gas flow cryostat. The sample is mounted
between a ring and a sphere [Fig. 1(b)] and biaxial strain is
achieved by moving the sphere towards the ring [14]. The
film (much thinner than the substrate), which is located on
the upper side of the sample, undergoes a symmetric
biaxial tensile strain at the center of the ring. The strain
is approximately uniform within ~1 mm of diameter from
the center, which is of the order of the x-ray beam spot.

Figure 2(a) shows the x-ray diffraction patterns for the
130 nm MnAs film under different external stress condi-
tions at $T = 0\,^{\circ}C$. The diffraction peak corresponds to the
MnAs(004) reflection. When an external biaxial tensile
strain is applied to the MnAs films, the x-ray diffraction
peak shifts to higher angles, indicating a decrease of the
lattice parameter along the growth direction, due to the
stretching of the in-plane parameters. We also note a
decrease of the x-ray intensity for increasing strain. This
is attributed to a decrease of the probed volume, which

maintains the geometrical condition for a maximum of
diffraction as the sample curvature changes. We assumed
that the variation of the scattering structure factor with
strain is negligible since the strain range used in this
work is relatively small (less than 0.3%).

Figure 2(b) shows the x-ray diffraction spectra obtained
for temperatures ranging from zero to $60\,^{\circ}C$ during a
heating cycle without an external strain. The diffraction
patterns show two peaks: the lower one at $2\theta \sim 61^{\circ}$ cor-
responds to the α-MnAs phase and the peak at $2\theta \sim 62^{\circ}$
corresponds to the β-MnAs phase. At intermediate tem-
peratures, x-ray spectra exhibit both peaks, indicating the
coexistence of the two phases. Measurements for cooling
cycles give similar results with a small shift of the phase
transition to lower temperatures, resulting in a thermal
hysteresis, as observed in previous works [10].

Figure 3 shows the volume fraction F_α vs temperature of
the α-MnAs phase, with and without an external strain.
The fraction F_α was obtained from the ratio of the inte-
grated intensity of the α phase x-ray diffraction peak
relative to the sum of the total intensity of the peaks for
both α and β phases. F_α presents a nonabrupt profile with
a thermal hysteresis, as discussed before. Note that the
phase transition of the films starts at temperatures smaller
than that of the transition temperature of the bulk ($40\,^{\circ}C$).
When an external tensile strain is applied, the curves show
a clear shift to higher temperatures. We also observed very
similar results for a 160 nm MnAs/GaAs film. Because of
the phase coexistence across a large range of temperatures,
the phase-transition temperature is not well defined for the
film. Therefore, we choose to define a characteristic tran-
sition temperature, T_p, as the temperature where F_α is 0.5.

We present in Table I the lattice parameters of the MnAs
film, as grown and under external strain, and those of bulk
MnAs from the literature [15]. The lattice parameters of
the as-grown film were obtained from specular and grazing
incident diffraction (GID) measurements. In the case of the
film under an external strain, we have only measured the
parameter c_{ortho}, since the biaxial stress cell does not
allow GID measurements. In this case, we have derived
the other parameters using the relation between the in-
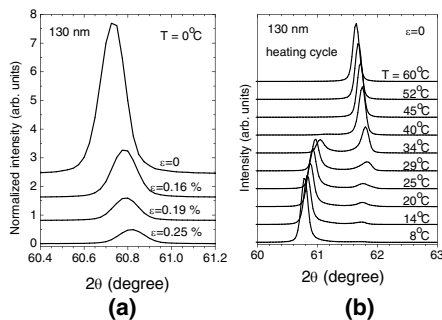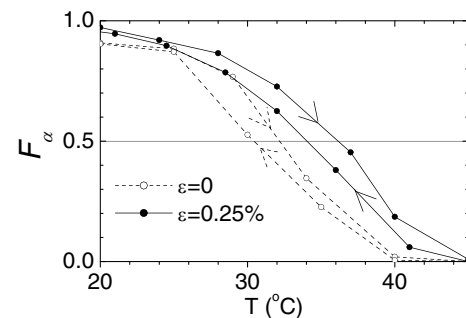

FIG. 2. (a) Biaxial tensile strain dependence of the x-ray
diffraction patterns for the MnAs/GaAs film. (b) Temperature
dependent x-ray diffraction patterns for the same sample without
an external strain.

FIG. 3. Temperature dependence of the volume fraction of
α-phase F_α of the 130 nm MnAs film.

TABLE I. Lattice parameters, unit cell volume (V), and relative temperature variation $\frac{\delta T_P}{T_P}$ of the 130 nm MnAs film and of MnAs bulk [15] in the α-MnAs phase for $T = 20\,°$C. In parenthesis the lattice parameter variation relative to bulk is shown. $\frac{\delta J_0}{J_0}$ are theoretical data.

	MnAs Bulk	film $\epsilon_\parallel = 0$	film $\epsilon_\parallel = 0.25\%$
a_{ortho} (Å)	5.706	5.764(+1.0%)	5.778(+1.27%)
b_{ortho} (Å)	3.724	3.710(−0.37%)	3.719(−0.13%)
c_{ortho} (Å)	6.450	6.440(−0.15%)	6.434(−0.25%)
V (Å³)	137.06	137.72(+0.48%)	138.26(+0.88%)
$\frac{\delta T_P}{T_P}$ (%)	0.0	−3.2	−1.6
$\frac{\delta J_0}{J_0}$ (%)	0.0	−3.0	−2.4

plane ($\epsilon_\parallel = \frac{\Delta a_{\text{ortho}}}{a_{\text{ortho}}} = \frac{\Delta b_{\text{ortho}}}{b_{\text{ortho}}}$) and out-of-plane ($\epsilon_z = \frac{\Delta c_{\text{ortho}}}{c_{\text{ortho}}}$) lattice parameter variations given by $\epsilon_\parallel = -[\frac{C_{12}+C_{23}}{C_{22}}]\epsilon_z$, where C_{ij} are the elements of the elastic constant tensor of MnAs [16]. For the condition of maximum strain applied to the sample we obtained from the x-ray measurements $\frac{\Delta c_{\text{ortho}}}{c_{\text{ortho}}} = 0.11\%$, which corresponds to $\frac{\Delta a_{\text{ortho}}}{a_{\text{ortho}}} = \frac{\Delta b_{\text{ortho}}}{b_{\text{ortho}}} = 0.25\%$. Comparing the lattice parameters between bulk and as-grown film, we observe that the MnAs film is stretched along the a_{ortho} direction and is shrunk in the hexagonal basal plane. Similar results were observed in a previous work [10]. The resulting unit cell volume in the film is 0.48% larger than that in the bulk and presents a smaller T_p. When the film is under external tensile strain, the unit cell volume shows a further increase (becoming 0.88% larger than the bulk). In this case, however, the increase of the cell volume is accompanied by an increase of T_p. Bean and Rodbell [1] have predicted an enhancement of T_p upon increasing the MnAs unit cell volume. Our results show, however, that T_p is not a simple function of the cell volume and it does depend on the lattice parameters in a more complex way.

In order to analyze our results, we have performed calculations based on the density functional theory (DFT) using the numerical implementation contained in the pseudopotential code SIESTA [17], and considering the generalized gradient approximation of the exchange correlation potential [18]. We used an s-p-d basis set for both Mn and As with double zeta polarized s and p orbitals and simple double zeta for the d orbitals. The cutoff radii of the first zetas are as follows: Mn $4s$ and $4p$ 7.5 bohr, Mn $3d$ 5.5 bohr, As $4s$, $4p$, and $4d$ 6 bohr. The second zeta cutoffs are determined with the split norm scheme [17]. Finally the real space mesh cutoff is 300 Ry and we considered 616 k points in the full B31 Brillouin zone. We analyzed several possible magnetic configurations for each lattice distortion, evaluating a Heisenberg-type expression for the total energy: $E_H = E_0 - \frac{1}{2}\Sigma_{i,j}J_{ij}\mathbf{s}_i \cdot \mathbf{s}_j$, where J_{ij} are the Heisenberg exchange parameters ($J_{ii} = 0$), E_0 is the total

energy of the paramagnetic state and $\mathbf{s}_i$ is the spin unit vector at site i. The coefficient J_{ij} depends solely on the separation vector $\mathbf{R}_{i,j}$ between spins i and j. The parameters $J_{(i,j)}$ were obtained by minimizing the difference between the total energy obtained from the DFT calculations and the Heisenberg energy, where couplings up to third nearest neighbors were considered. A detailed description of the calculations and of the fitting procedure will be presented elsewhere [19]. The parameter $J_0 = \Sigma_j J_{0j}$, which in the mean field approximation is proportional to the Curie temperature, is a measure of the stability of the ferromagnetic phase [1,19,20]. The larger the gain in magnetic energy, the higher should be T_p. As a first approximation, we assume that the change of T_p is proportional to the equivalent change of J_0: $\frac{\delta T_p}{T_p} = \frac{\delta J_0}{J_0}$. Table I gives the calculated values of $\frac{\delta J_0}{J_0}$ for the film, with and without an external stain, and its relative change with respect to the bulk. We observe that the calculated values of $\frac{\delta J_0}{J_0}$ are in very good agreement with the corresponding experimental values of $\frac{\delta T_p}{T_p}$ for the as-grown sample. The agreement is not equally good for the film under external biaxial strain. In this case the in-plane parameters were calculated from the out-of-plane one using the elastic tensor, which carries a significant experimental uncertainty. We remark, in particular, that the theory correctly predicts the direction of the transition temperature changes due to the film distortions: a decrease of T_p from bulk to the as-grown film and a partial recovery of T_p when a biaxial tensile strain is applied to the film.

In order to accomplish a more general analysis, we may consider that for small distortions J_0 is linearly dependent on the orthorhombic lattice parameters [same notation of the Fig. 1(a)]:

$$\frac{\delta J_0}{J_0} = K_a \frac{\delta a}{a} + K_b \frac{\delta b}{b} + K_c \frac{\delta c}{c},$$

where K_a, K_b, and K_c are constants that can be determined by calculating J_0 for various distorted cells and fitting the results using the linear relationship expressed above. Following this procedure we observed a well-behaved linear dependence from which we obtained:

$$K_a = -1.0, \qquad K_b = 5.2, \qquad K_c = 4.2.$$

The results clearly show that stretching the unit cell along the basal plane raises T_p (since K_b and $K_c > 0$), while stretching along the a axis lowers T_p ($K_a < 0$). We point out that the distortion of a single lattice parameter alters the value of various distances between atoms in a complex way, so that the constants K_i reflect the combination of all those changes. We observed that an increase of the separation between Mn atoms (including the distance between nearest Mn neighbors and the Mn-Mn separation in the

P H Y S I C A L   R E V I E W   L E T T E R S

basal plane) results in an increase of T_p, while an increase of the separation between Mn and As atoms results in a decrease of T_p [19]. When the cell is stretched along the a_{ortho} axis, the increase of the Mn-As separations slightly dominates, resulting in a small negative value for K_a. For distortions along the b_{ortho} and c_{ortho} axes, the increase of the Mn-Mn separation strongly dominates so that K_b and K_c are positive.

We may now interpret our experimental results. The strain effects of growing a MnAs thin film with the A orientation on GaAs results in the stretching of the a_{ortho} axis and the contraction of both the b_{ortho} and c_{ortho} axes. All these distortions contribute to reduce T_p. When an external biaxial stress is applied along the film plane, the lattice parameters a_{ortho} and b_{ortho} increase while the c_{ortho} parameter decreases. The net result is a small enhancement of T_p, reflecting the balance of the K parameters and the relative large value of K_b. Our calculations also explain why a hydrostatic pressure lowers the phase-transition temperature of bulk MnAs, as observed in previous works [1]. Under hydrostatic pressure, the b_{ortho} and c_{ortho} parameters suffer a stronger contraction than a_{ortho} due to the anisotropy of the MnAs elastic constant tensor [16]. This effect, combined with the fact that $|K_b|$ and $|K_c|$ are bigger than $|K_a|$, results in a decrease of T_p.

In summary, based on our results, we propose that higher T_p can be achieved by growing MnAs in such a way to maximize the lattice parameters of the basal plane and minimize the lattice parameter in the perpendicular direction. Finally, the possibility of moving across the phase-transition temperature by applying an external biaxial pressure opens a new avenue to mechanically driven magneto-devices. One can envision composite materials comprising MnAs and piezoelectric compounds, where the magnetism can be mechanically switched on and off.

---

*Electronic address: iikawa@ifi.unicamp.br
[1] C. P. Bean and D. S. Rodbell, Phys. Rev. **126**, 104 (1962).
[2] V. A. Chernenko et al., J. Appl. Phys. **85**, 7833 (1999).
[3] S. Gama et al., Phys. Rev. Lett. **93**, 237202 (2004).
[4] M. Tanaka et al., Appl. Phys. Lett. **65**, 1964 (1994).
[5] M. Ramsteiner et al., Phys. Rev. B **66**, 081304(R) (2002).
[6] K. Motizuki and K. Katoh, J. Phys. Soc. Jpn. **53**, 735 (1984).
[7] V. M. Kaganer et al., Phys. Rev. Lett. **85**, 341 (2000).
[8] T. Plake et al., Appl. Phys. Lett. **80**, 2523 (2002).
[9] M. Kästner et al., J. Appl. Phys. **92**, 5711 (2002).
[10] F. Iikawa et al., Appl. Phys. Lett. **85**, 2250 (2004).
[11] N. Menyuk et al., Phys. Rev. **177**, 942 (1969).
[12] S. Sanvito and N. A. Hill, Phys. Rev. B **62**, 15553 (2000).
[13] F. Schippan et al., J. Vac. Sci. Technol. B **17**, 1716 (1999).
[14] M. P. F. Godoy et al., Rev. Sci. Instrum. **75**, 1947 (2004).
[15] B. T. M. Willis and H. P. Rooksby, Proc. Phys. Soc. London, Sect. B **67**, 290 (1954).
[16] M. Dörfler and K. Bärner, Phys. Status Solidi A **17**, 141 (1973).
[17] J. M. Soler et al., J. Phys. Condens. Matter **14**, 2745 (2002).
[18] J. P. Perdew, K. Burke, and M. Ernzerhof, Phys. Rev. Lett. **77**, 3865 (1996).
[19] I. Rungger and S. Sanvito (to be published).
[20] T. Kato, K. Nagai, and T. Aisaka, J. Phys. C **16**, 3183 (1983).